Wave Trains Excited by Cross-Equatorial Passage of the Monsoon Annual Cycle

T. N. KRISHNAMURTI, C. P. WAGNER, TINA J. CARTWRIGHT, AND DARLENE OOSTERHOF

Department of Meteorology, The Florida State University, Tallahassee, Florida

29 July 1996 and 11 February 1997

ABSTRACT

In this paper the authors illustrate wave trains that are excited during the equatorial passage of the annual cycle of monsoonal convection. Twice a year, during roughly the months of December–January and March–April, the annual cycle of monsoonal convection crosses the equator. A principle axis of annual cycle monsoon precipitation extends from the Java Sea to the eastern Himalayas. Monsoonal convection makes a north–south seesaw roughly along this axis each year. Near-equatorial convection provides a tropospheric heat source somewhat akin to that of El Niño over the equatorial Pacific Ocean. This equatorial passage of the monsoonal heat source excites a wave train, somewhat similar to the familiar Pacific–North American pattern. Monsoonal wave trains were extracted from a 9-yr dataset, and a composite geometry was constructed. This note also illustrates excitation of short-period wet and dry spells associated with excitation of this wave train. This is illustrated for several trough and ridge locations of the wave train by examining rainfall for a sequence of days some 10 days prior to and 10 days subsequent to passage of this wave train. There is a strong suggestion that equational passage of monsoon convection does influence short-term dry and wet spells along the wave train; that is, beneath upper troughs (ridges), wet (dry) weather prevails.

1. Introduction

The monsoon annual cycle includes north–south migration of a rainbelt from Indonesia (in the northern winter) to the eastern Himalayas (in the northern summer). This monsoon annual cycle includes the migration of the ITCZ between the Southern and Northern Hemispheres across the equator during late fall and spring (a list of acronyms is presented in Table 1). A tropospheric heat source resides close to the equator during this period of cross-equatorial migration. The annual cycle of monthly mean climatological monsoon rainfall is illustrated in Fig. 1, where cross-equatorial migration is clearly evident. This illustration is based on voluminous data collection efforts at NCAR (principally by D. Shea) and includes a dense collection of surface rain gauge data and oceanic rainfall based on satellite OLR algorithms. This climatology clearly illustrates meridional passage of a rainfall axis through the annual cycle. Along this axis (marked by a red line) we note some zonal variability. Maximum rainfall rates on the order of 400 mm per month are noted along this axis. It is possible that the ITCZ does not physically cross the equator. It propagates meridionally toward the equator in one hemisphere and away from the equator in the other hemisphere. For all intents and purposes, we can regard this as an equatorial crossing of the rainbelt and the heat source without any essential violation of the results presented here. What matters is the presence of a heat source in the vicinity of the equator for the excitation of the wave trains.

Monsoonal rainfall exhibits equatorial crossings during December–January and March–April. During December–January the winter monsoon rainfall axis migrates south toward northern Australia, whereas during March–April the axis of maximum rainfall makes its northward excursion toward central Malaysia as the summer monsoon becomes established over Asia.

This type of equatorial convection is similar to what one sees during El Niño events over the central Pacific Ocean. The similarity of the heat source among the equatorial crossing of the monsoon rainfall of the El Niño is primarily based on rainfall observations, both of which are of the order of 1000 mm per month. Thus we expect the heat source related to deep cumulus convection to be of a similar magnitude. The El Niño–related deep tropospheric heat source is known to excite

TABLE 1. List of acronyms.

ITCZ	Intertropical convergence zone
NCAR	National Center for Atmospheric Research
OLR	Outgoing longwave radiation
PNA	Pacific–North American pattern
TIROS-N	*Thermal Infrared Orbiting Satellite-N*
MSU	Microwave sensing unit

Corresponding author address: Dr. T. N. Krishnamurti, Dept. of Meteorology, B-161, The Florida State University, 430 Love Building, Tallahassee, FL 32306-3034.
E-mail: tnk@cloud1.met.fsu.edu

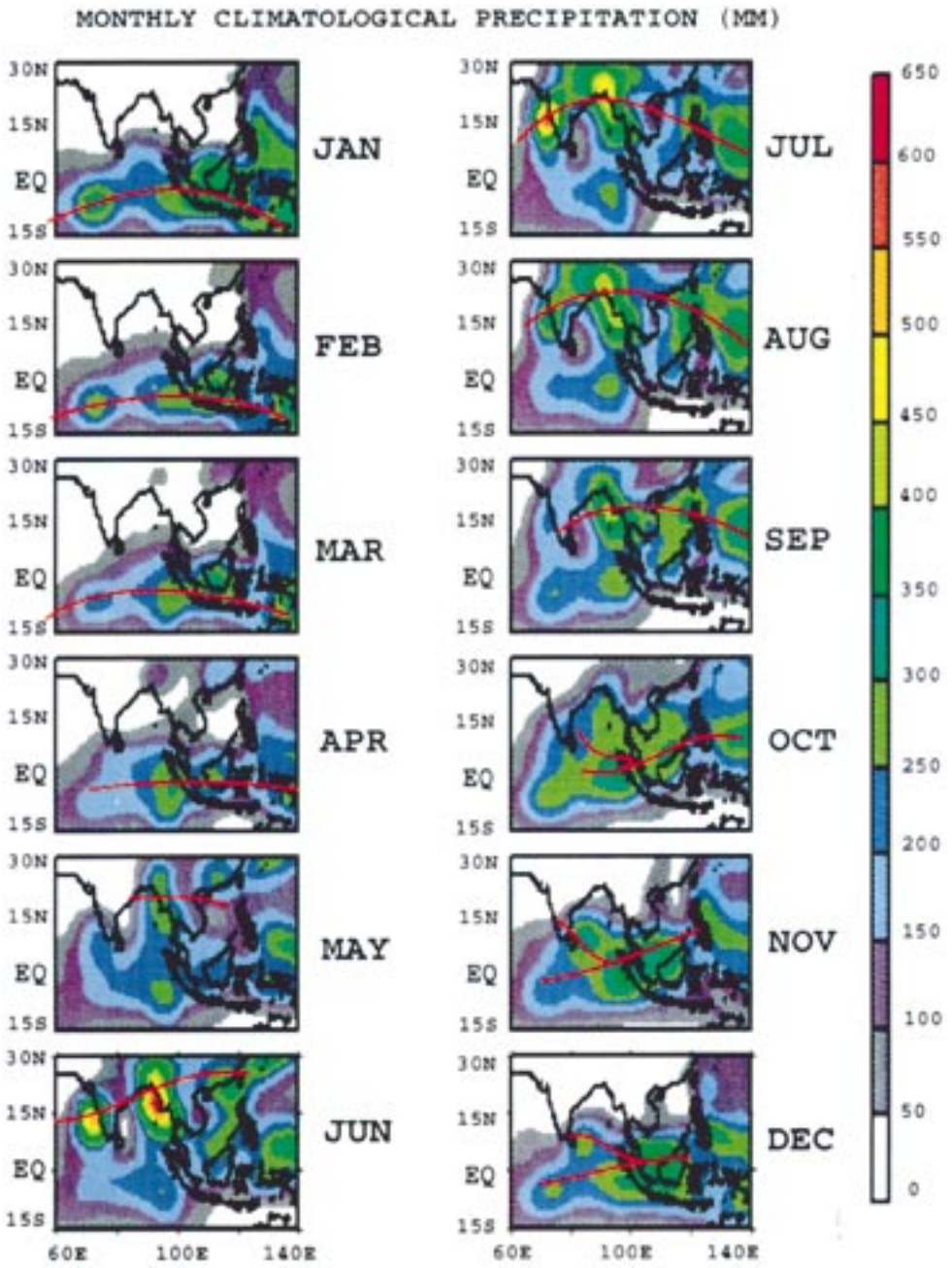

FIG. 1. Monthly mean climatological rainfall (mm month^{-1}) for the entire year over the monsoon region. This is based on 30 yr of data from 1950 through 1979 provided by D. Shea of NCAR. The red line denotes the time the maximum migrates across the equator (around December–January and March–April).

a wave train identified as the familiar PNA pattern (Wallace and Gutzler 1981).

Nitta (1986, 1987) and Lau (1992) have noted winter season wave trains that originate south of Japan and traverse across the Pacific toward North America. These are usually identified as negative PNA wave trains that are observed during La Niña years. The source of excitation of these negative PNA wave trains has not been very clear. They may be related to dynamical instabilities (Palmer 1988). These are not just related to equatorial crossing of monsoon convection.

Given that similarity in near-equatorial tropospheric heat sources for the cross-equatorial migration of the monsoon and for the El Niño, one can perhaps expect similar wave trains as the PNA emanating from the monsoon migration region. In this note we show that by averaging 300-mb geopotential heights in a simple manner we can in fact illustrate this wave train from observations.

2. Monsoon wave trains

It is customary to illustrate wave trains from time-averaged upper-tropospheric geopotential heights. Climatology of the seasonal monsoon carries a substantial portion of the total annual geopotential height variance. In order to best illustrate transient wave trains generated by equatorial crossing of a monsoon heat source, it was felt that removal of seasonal climatology may easily differentiate the atmospheric structure prior to the equator crossing with the atmospheric structure subsequent to the equatorial crossing of deep convection. We felt that both of the above objectives could be achieved by subtracting geopotential heights at 300 mb for day -10 from day $+10$ (where day 0 denotes the date of equatorial crossing of deep convection); that is,

$$Z_{10} = \bar{Z} + Z'_{-10}$$

$$Z_{+10} = \bar{Z} + Z'_{+10},$$

hence,

$$Z_{10} - Z_{-10} = Z'_{10} - Z'_{-10} = \Delta Z,$$

where Z_{10} denotes geopotential heights 10 days after equatorial crossing and Z_{-10} denotes the same 10 days prior to equatorial crossing. The overbar denotes climatological geopotential heights; the prime denotes departure from climatology. An example of the equational crossing is illustrated in Fig. 2. Here we used low values of OLR to represent tropical convection. This covers the period 1 November 1982–31 January 1983. We performed a daily zonal average of net OLR (W m^{-2}) across longitudes 50°–110E and show passage of minimum OLR on a latitude–time diagram. Equatorial passage for this case occurs around 25 November 1982. We have used such an arrow in Fig. 2 to identify equational crossing date.

Figure 3a shows several wave trains that emanate

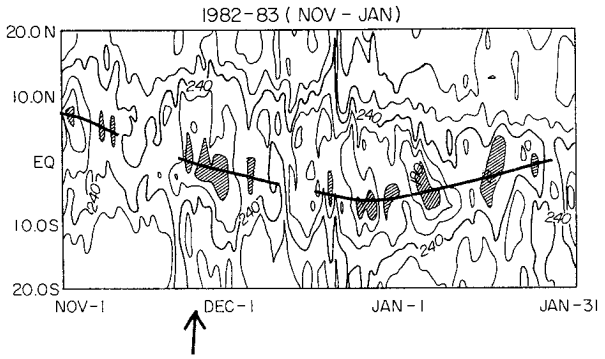

FIG. 2. A latitude–time diagram showing the equational crossing of minimum outgoing longwave radiation during winter 1982/83. Zonal average covers the longitude 50°–110°E.

from the Indian Ocean. Here we illustrate the geopotential height composite differences; namely, $\Delta Z = Z'_{10} - Z'_{-10}$. It defines the wave trains very clearly for numerous years. The ΔZ gradient in the immediate vicinity of the equatorial heat source, near 5°–10°N, is positive (but weak) in all cases. A pronounced feature is the appearance of a negative height difference located over northern India. The amplitude of this center is on the order of 100 m. Here, ΔZ is also displayed for the years 1981–84 and 1987. The ΔZ's for 1985 and 1986 were quite similar to those for 1984. In 1982 we noted an oscillating pattern of equatorial crossing, that is, one appearing around 29 November and another around 2 December. Both fields are shown to illustrate an essential robustness of these results. In this sequence there were two El Niño years, 1982 and 1987. Monsoonal wave trains appeared to be disrupted over the central Pacific Ocean. The years 1982 and 1983 cover an El Niño and a post–El Niño year. The El Niño–related east–west overturnings can offset some of the features of the equatorial crossing wave trains, especially over Asia. Thus we may not expect to see similar behavior in those two years (Fig. 3a). The southward displacement of the equatorial wave train over South Korea in 1982 may be a consequence of the El Niño teleconnection. One might wonder about the statistical significance of the wave train shown in Fig. 4 since it includes two El Niño years. However, the fact that a well-marked wave train remains in this averaging (similar to what was seen for the non–El Niño years) is encouraging. We have also examined wave trains during the northward seasonal migration of the monsoon, that is, during March and April. We noted that as monsoon rainfall migrates from the Southern to the Northern Hemisphere during March and April a similar wave train propagates south over the Southern Hemisphere from the monsoon region. Figure 3b illustrates some of these examples based on equational crossings. To see monsoonal wave train patterns more clearly, we composited ΔZ patterns in Fig. 3a for all of the years from 1981 through 1987. The composite wave train stands out very clearly (Fig. 4a). The composite wave

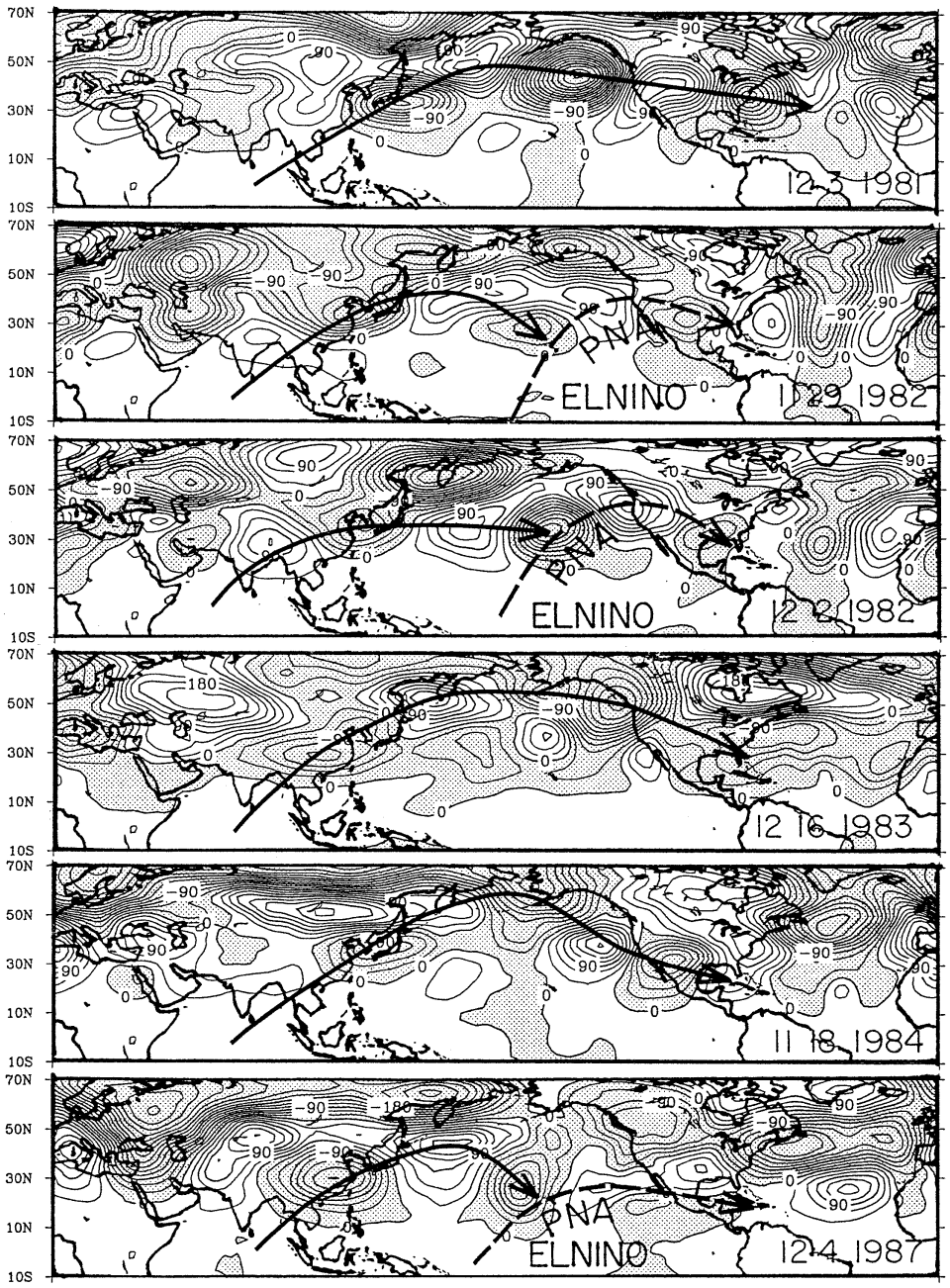

FIG. 3a. The 300-mb geopotential anomalies for six cases (30-gpm contour intervals) showing southward passage of the monsoon rain across the equator. Shaded regions represent negative values. Case data is given in the lower-left side of each box. The solid arrow represents the wave train, while the dashed arrow represents the El Niño–driven PNA pattern.

train can be seen for the southern propagating case in Fig. 4b. In Fig. 4b we show the wave trains during fall equatorial crossing (the descending node) of the equatorial convection. This appears to be an interesting counterpart of Fig. 4a. Geopotential height anomalies 10 days subsequent to equatorial passage appear to be distinctly different from geopotential anomalies 10 days prior to passage since these denote amplification of upper troughs and ridges at 300 mb between 10° and 30°N. Thus, we can expect to see some modulation of weather beneath these upper-air systems on this timescale.

The wave train emanates from the Tropics into subtropical and middle latitudes. Troughs and ridges of this system have rising and sinking patterns similar to those in most quasigeostrophic weather systems. Thus we can expect to see a precipitation signature closely coupled with

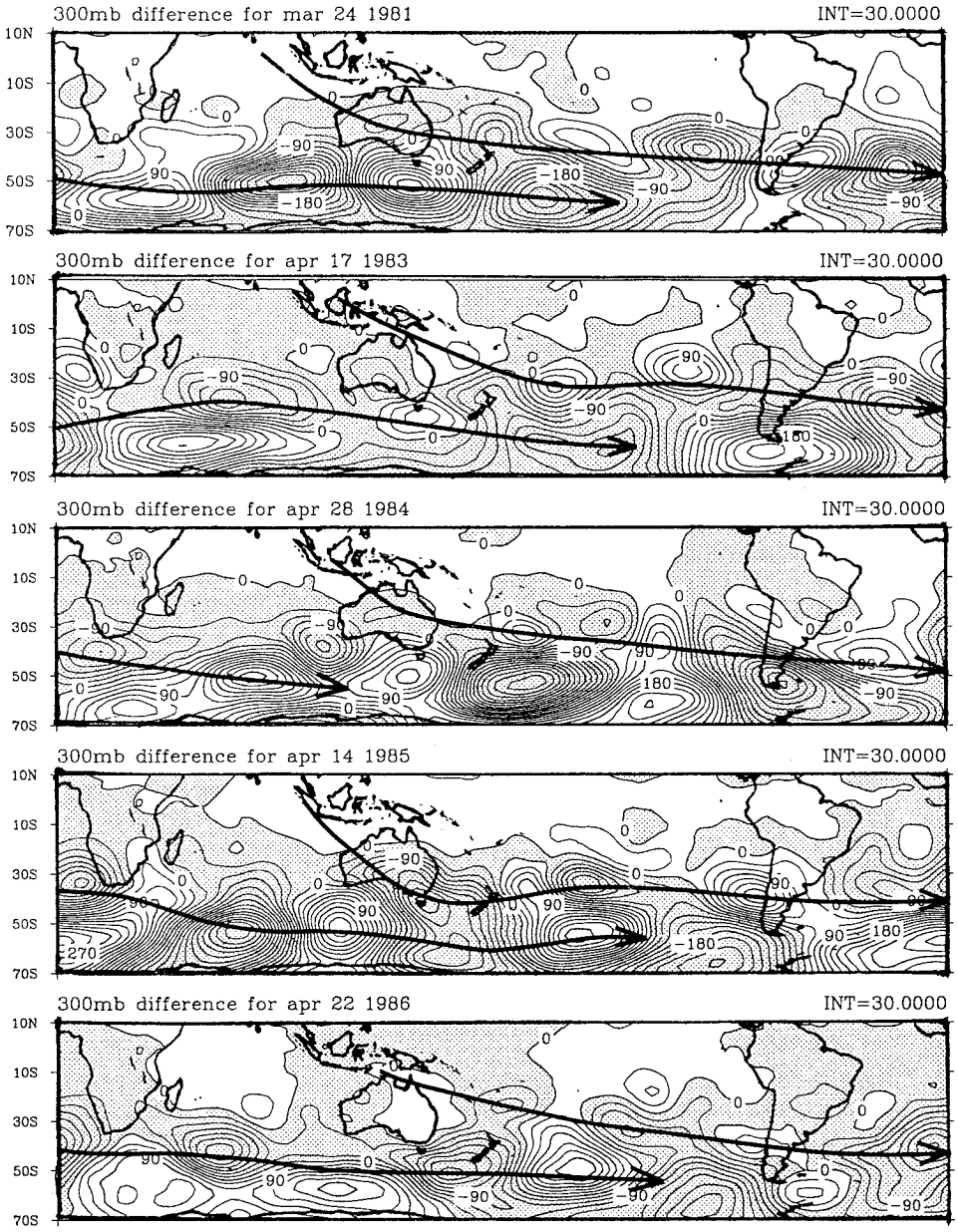

FIG. 3b. As in Fig. 3a except for northward passage of monsoon rain across the equator.

the geopotential height wave trains. Wave trains were examined using Spencer's global oceanic precipitation datasets (Spencer 1993), available on a 2.5° grid from an MSU provided on board *TIROS-N* satellites. Precipitation data cover the period 1979–91. Precipitation is calibrated in two ways. First it is intercalibrated between satellites, and then it is calibrated using rain gauge measurements. Rain gauge measurements consist of data from 5 to 10 years of globally distributed low-elevation island and coastal rain accumulation measurements from 132 gauges. A similar wave train was not evident when the datasets centered around day −10 were composited.

Figure 5 illustrates a composite ocean rainfall distribution from this dataset for two cases. This composite includes cases covered in Fig. 3a. Here we have subtracted precipitation at day −10 from precipitation at day +10 for all cases prior to averaging. Precipitation signatures typically show alternating wet and dry regions along the wave train. Basically the region east of the wave train upper trough tends to be wet. The converse is noted west of the upper trough. This is not surprising since these are robust midlatitude trough–ridge patterns. An implication of this result is a transient climate over the east China coast; we have noted wet spells during upper trough conditions over eastern China in association with equatorial passage of convection. During periods when well-estab-

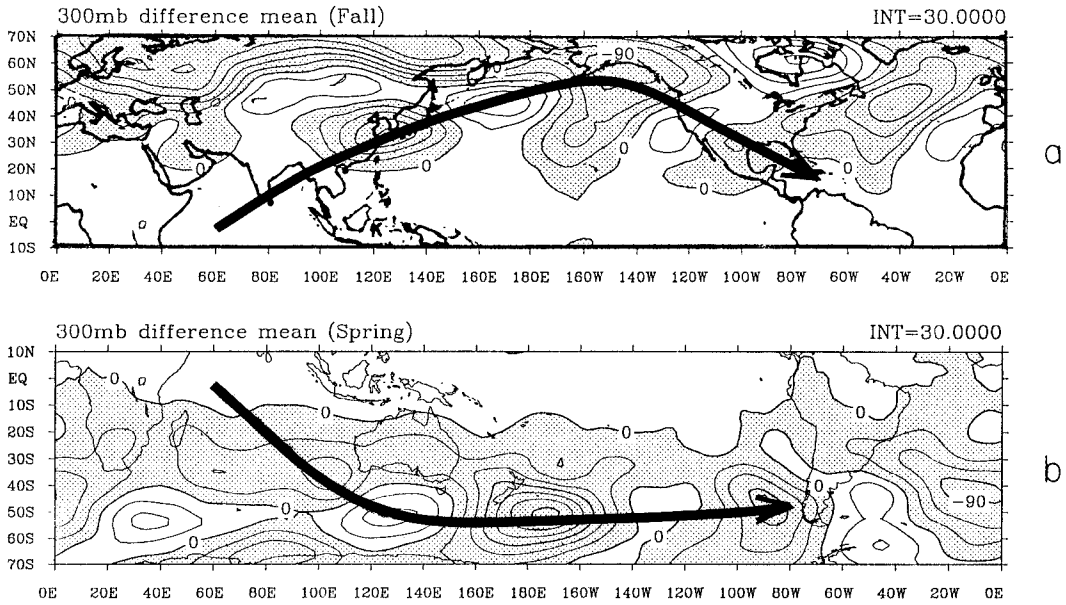

FIG. 4. (a) Composite mean of the cases shown in Fig. 3a. (b) Composite mean of the cases shown in Fig. 3b.

lished wave trains were present, we noted the presence of stationary fronts and frontal cyclones, along with extensive cloud cover and heavy precipitation along the east China coast.

3. Concluding remarks

The PNA pattern was brought to the attention of the climate community by Wallace and Gutzler (1981); that is, a stationary wave train attributed to a Rossby wave response to an equatorial heat source (deep cumulus convection) during El Niño. This wave train follows a great-circle route, emanating from the central equatorial Pacific, going as far north as southwestern Canada and terminating over the southeastern United States. The annual cycle of monsoon convection crosses the equator twice a year, during December–January and during March–April. We show that this equatorial passage of deep convection/heavy rain does indeed excite a wave train that emanates from these convective regions and traverses roughly a great-circle route. We have examined 9 years of geopotential height and OLR data. Furthermore, we have used oceanic daily rainfall from the recent datasets produced by Spencer to confirm the wave

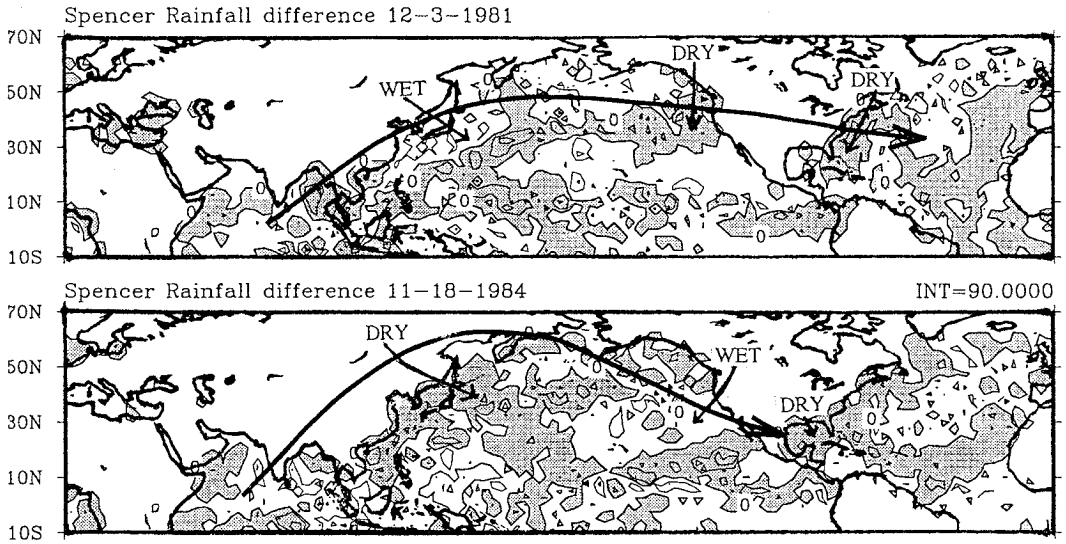

FIG. 5. Difference in rainfall (mm day^{-1}) (plus 10 days minus minus 10 days) between equatorial crossing of monsoon rainfall designated at day 0 for the December 1981 case where shaded areas represent dry regions. The H's and L's represent ridge and trough locations, respectively.

train and associated rainfall. Similar wave trains could perhaps be excited during the meridional passage of the rainfall belts across the equator over the Congo and Brazil. We have not explored these issues here. Modeling studies are needed to ascertain that these wave trains are indeed excited by the meridional passage of deep convection. Such studies are being carried out.

Acknowledgments. Research reported here was supported by NOAA Grant NA-16RC0358-03 and NSF Grant ATM 9312537. Computations for this work were carried out on the CRAY Y-MP at the National Center for Atmospheric Research, Boulder, Colorado. The NCAR facility is sponsored by the National Science Foundation.

REFERENCES

Lau, K. M., 1992: East Asian summer monsoon variability and climate teleconnection. *J. Meteor. Soc. Japan,* **70,** 211–242.

Nitta, T., 1986: Long term variations of cloud amount in the western Pacific region. *J. Meteor. Soc. Japan,* **64,** 373–390.

——, 1987: Convective activities in the tropical western Pacific and their impact on the Northern Hemisphere circulation. *J. Meteor. Soc. Japan,* **65,** 373–390.

Palmer, T. N., 1988: Medium and extended range predictability and stability of the Pacific/North American mode. *Quart. J. Roy. Meteor. Soc.,* **114,** 691–713.

Spencer, R. W., 1993: Global oceanic precipitation from MSU during 1979–91 and comparison to other climatologies. *J. Climate,* **6,** 1301–1326.

Wallace, J. M., and D. S. Gutzler, 1981: Teleconnections in the geopotential height field during the Northern Hemisphere winter. *Mon Wea. Rev.,* **109,** 784–812.